being followed by a thicker but coherent vortex that attains 70% of the freestream axial velocity at its center before it spirals away from the axis and begins to dissipate. The helical vortex spirals around a large region of reversed flow which begins at 55% of root chord and extends downstream of the trailing edge of the wing.

The reformation of the vortex downstream of breakdown, although not typical of delta wing flows, has been noted in experiments and calculations of breakdown in swirling pipe flows.[12,13] The coarse mesh solution shows no indication of the bubble breakdown, which suggests that further differences could appear with additional refinement.

V. Conclusion

An adaptive mesh Euler solver was used to simulate the flow over a sharp edged delta wing. Adaptation enables the normal force to be well predicted at high range of angle of attack in the prescence of vortex breakdown. The position of breakdown is in reasonable agreement with experimental measurements. Vortex breakdown is predicted to primarily exhibit the spiral form, which is typically observed in delta wing experiments.

Acknowledgments

This work was supported by Air Force Office of Scientific Research Contract AFOSR-89-0395A, monitored by L. Sakell; and by the McDonnell Aircraft Company under MDC/MDRL IRAD Sponsorship. The authors would like to thank Jaime Peraire of Massachusetts Institute of Technology, Ken Morgan of University College, Swansea, Wales, and Joaquin Peiró of the Imperial College of Science, Technology, and Medicine, London, England, for the use of the mesh generation system.

References

[1]Lambourne, N. C., and Bryer, D. W., "The Bursting of Leading-Edge Vortices—Some Observations and Discussions of the Phenomenon," Aeronautical Research Council, R & M 3283, 1961.

[2]Modiano, D. L., "Adaptive Mesh Euler Equation Computation of Vortex Breakdown in Delta Wing Flow," Ph.D. Thesis, Massachusetts Inst. of Technology, Cambridge, MA, Feb. 1993; also Massachusetts Inst. of Technology Computational Aerospace Sciences Lab. Rept. CASL-TR-93-001, Cambridge, MA, Jan. 1993.

[3]Peraire, J., Morgan, K., and Peiró, J., "Unstructured Finite Element Mesh Generation and Adaptive Procedures for CFD," *Application of Mesh Generation to Complex 3-D Geometries*, AGARD-CP-464, May 1989.

[4]Holmes, D. G., and Connell, S. D., "Solution of the 2D Navier-Stokes Equations on Unstructured Adaptive Grids," AIAA Paper 89-1932, June 1989.

[5]Jameson, A., Schmidt, W., and Turkel, E., "Numerical Solutions of the Euler Equations by Finite Volume Methods Using Runge-Kutta Time-Stepping Schemes," AIAA Paper 81-1259, June 1981.

[6]Giles, M. B., "Energy Stability Analysis of Multi-Step Methods on Unstructured Meshes," Massachusetts Inst. of Technology Computational Fluid Dynamics Lab. Rept. CFDL-TR-87-1, Cambridge, MA, March 1987.

[7]Borsi, M., Formaggia, L., Hettena, E., Santillan, S., Selmin, V., and Tarditi, S., "Vortical Flow Simulation by Using Structured and Unstructured Grids," *Vortex Flow Aerodynamics*, AGARD-CP-494, Oct. 1990.

[8]Melton, J. E., Thomas, S. D., and Cappucio, G., "Unstructured Euler-Flow Solutions Using Hexahedral Cell Refinement," AIAA Paper 91-0637, Jan. 1991.

[9]Ekaterinaris, J. A., and Schiff, L. B., "Vortical Flows Over Delta Wings and Numerical Prediction of Vortex Breakdown," AIAA Paper 90-0102, Jan. 1990.

[10]Jarrah, M. A., "Unsteady Aerodynamics of Delta Wings Performing Maneuvers to High Angle of Attack," Ph.D. Thesis, Stanford Univ., Stanford, CA, Dec. 1988.

[11]Hummel, D., and Srinivasan, P. S., "Vortex Breakdown Effects on the Low-Speed Aerodynamic Characteristics of Slender Delta Wings in Symmetrical Flow," *Royal Aeronautical Society Journal*, Vol. 71, April 1967, pp. 319–322.

[12]Sarpkaya, T., "On Stationary and Travelling Vortex Breakdowns," *Journal of Fluid Mechanics*, Vol. 45, Feb. 1971, pp. 545–559.

[13]Lopez, J. M., "Axisymmetric Vortex Breakdown, Part 1. Confined Swirling Flow," *Journal of Fluid Mechanics*, Vol. 221, Dec. 1990, pp. 533–552.

Numerical Computations of Supersonic Base Flow with Special Emphasis on Turbulence Modeling

Jubaraj Sahu*
U.S. Army Research Laboratory,
Aberdeen Proving Ground, Maryland 21005

Introduction

ONE of the important parameters in the design of shells is the total aerodynamic drag. The base drag component is a large part and can be as high as 50% or more of the total drag. Therefore, it is necessary to predict the base pressure as accurately as possible. The ability to compute the base region flowfield for projectiles using Navier-Stokes computational techniques has been developed.[1] This capability is very important for determining aerodynamic coefficient data including the total aerodynamic drag. A number of base flow calculations have been made, and base drag and total drag have been predicted with reasonable accuracy. However, due to the lack of available data, the base flow predictive capabilities have not been assessed with detailed base pressure distribution, mean flow velocity components, and turbulence quantities. This is especially true of the base flow for axisymmetric bodies at transonic and supersonic speeds. Recently, experimental measurements[2] have been made in the base region for supersonic flow over a cylindrical afterbody. The data includes base pressure distribution (over the base), mean flow, as well as turbulence quantities.

Figure 1 is a schematic diagram showing the important features of supersonic base flow. The approaching supersonic turbulent boundary layer separates at the base corner, and the free shear layer region is formed in the wake. The flow expands at the base corner and is followed by the recompression shock downstream of the base which realigns the flow. The flow then redevelops in the trailing wake. A low-pressure region is formed immediately downstream of the base which is characterized by a low-speed recirculating flow region. Interaction between this recirculating region and the inviscid external flow occurs through the free shear mixing region. This is the region where turbulence plays an important role. The basic configuration used in this study is a cylindrical afterbody. Numerical flowfield computations have been performed at $M_\infty = 2.46$ and at 0-deg angle of attack. Various turbulence models (two algebraic models and a two-equation model) are used in the base flow region. Details of the flowfield such as Mach number contours and base pressure distributions are presented. Computed base pressure distributions are compared with available experimental data for the same conditions and the same configuration.

Turbulence Models

The complete set of time-dependent, Reynolds-averaged, thin-layer Navier-Stokes equations is solved numerically using an implicit finite-difference scheme. For turbulent base flow calculations, two algebraic models (Baldwin and Lomax[3] and Chow[4]) and a two-equation k-ε eddy viscosity turbulence model have been used.

Baldwin-Lomax Model

This is a two-layer model in which an eddy viscosity is calculated for an inner and an outer region. The inner region follows the Prandtl-Van Driest formulation. In both the inner and outer formulations, the distribution of vorticity is used to determine the length scales, thereby avoiding the necessity of finding the outer edge of the boundary layer.

Presented as Paper 92-4352 at the AIAA Atmospheric Flight Mechanics Conference, Hilton Head, SC, Aug. 10–12, 1992; received May 12, 1993; revision received Jan. 2, 1994; accepted for publication Jan. 3, 1994. This paper is declared a work of the U.S. Government and is not subject to copyright protection in the United States.

*Aerospace Engineer. Associate Fellow AIAA.

Chow Model

Another algebraic model that has been used in some of our base flow computations is that due to Chow.[4] This model is intended to be used in the base or wake region only. It is based on the simple exchange-coefficient concept. The turbulent eddy viscosity coefficient is usually given by $\mu_t = (1/4\sigma^2)xu_e$ where x is the distance measured from the origin of the mixing region (i.e., the base), u_e is the velocity at the edge of the mixing region, and σ is the spread rate parameter. It is known that σ assumes a value of 12 for an incompressible flow and it increases slightly with Mach number.

Two-Equation k-ε Model

The two-equation turbulence model used here is Chien's[5] k-ε model. In this model, two transport equations are solved for the two variables, k (turbulent kinetic energy) and ε (turbulent dissipation rate).

$$\rho\frac{Dk}{Dt} = \frac{\partial}{\partial X_j}\left[\left(\frac{\mu_t}{\sigma_k}+\mu\right)\frac{\partial k}{\partial X_j}\right] + \mu_t\frac{\partial u_i}{\partial X_j}\left(\frac{\partial u_i}{\partial X_j}+\frac{\partial u_j}{\partial X_i}\right) - \rho\varepsilon - 2\mu\frac{k}{y_n^2}$$

$$\rho\frac{D\varepsilon}{Dt} = \frac{\partial}{\partial X_j}\left[\left(\frac{\mu_t}{\sigma_\varepsilon}+\mu\right)\frac{\partial \varepsilon}{\partial X_j}\right] + c_1\mu_t\frac{\varepsilon}{k}\frac{\partial u_i}{\partial X_j}\left(\frac{\partial u_i}{\partial X_j}+\frac{\partial u_j}{\partial X_i}\right) - c_2\rho\frac{\varepsilon^2}{k} - 2\mu\frac{\varepsilon}{y_n^2}e^{-y^+/2}$$

The k-ε model employs the eddy viscosity concept and relates the turbulent eddy viscosity to k and ε by $\mu_t = c_\mu\rho(k^2/\varepsilon)$. This constitutes a low Reynolds number formulation of the k-ε model. Calculations are extended up to the wall itself, and exact values of the dependent variables at the wall are used as boundary conditions.

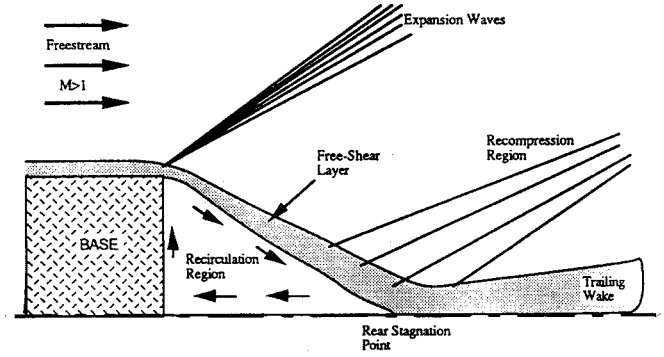

Fig. 1 Schematic diagram of supersonic base flow.

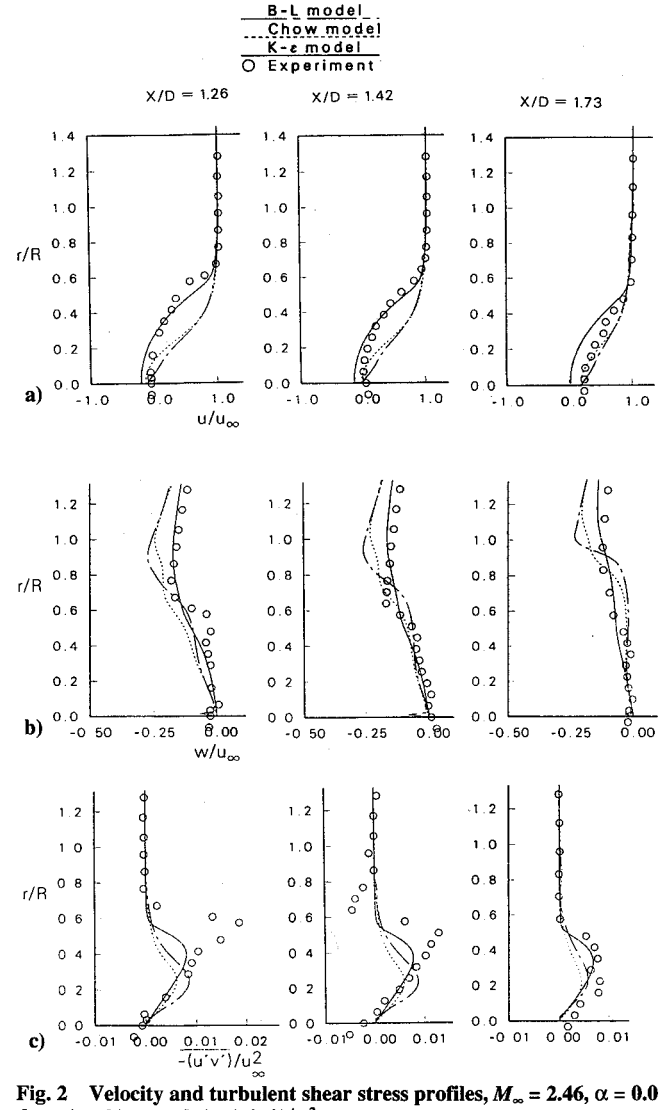

Fig. 2 Velocity and turbulent shear stress profiles, $M_\infty = 2.46$, $\alpha = 0.0$ deg: a) u, b) w, and c) $-(u'v')/u_\infty^2$.

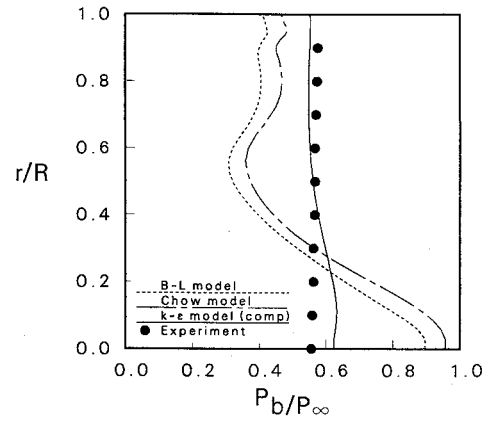

Fig. 3 Base pressure distribution, $M_\infty = 2.46$, $\alpha = 0.0$ deg.

Results

Experimental measurements[2] for this model have been made at the University of Illinois supersonic wind tunnel. The model was tested at Mach number of 2.46, 0-deg angle of attack and a Reynolds number of 5.21×10^7 per meter. In addition to measuring the velocity components at a few selected longitudinal positions in the wake or base region, the base pressure was measured at 19 positions over the base. The velocity profile was also measured at a station upstream of the base which provided the upstream boundary condition for base region flowfield calculations.

The computational grid consisted of 12,600 points. Grid points were clustered in the free shear layer and near the body walls. Because the k-ε calculations contain the low-Reynolds-number terms, two different small spacings were used near the base wall. The first one resulted in $y^+ \approx 3$ at the base wall near the centerline. The grid spacing was further refined to obtain $y^+ \approx 0.80$. No significant changes were observed in the results, including the base pressure. Figures 2a and 2b show the velocity components in the streamwise and normal directions. These velocity profiles are taken at three longitudinal positions in the wake or the base region (X/D = 1.26, 1.42, and 1.73). Here X is measured from the base downstream and r is the radial distance measured from the centerline of symmetry (D = base diameter and R = base radius). The computed velocity profiles obtained using the two algebraic turbulence models and the two-equation k-ε model are compared with the experimental data. In general, the u profiles obtained with the k-ε model are in much better agreement with the experiment in the shear layer regions for $X/D = 1.26$ and $X/D = 1.42$. The profiles are rather poorly predicted by both of the algebraic models at these two stations. The reattachment point estimated from the experimental measurements is about 1.4 base diameters downstream of the base. The

value computed with the k-ε model is 1.5. This small disagreement is also seen in the flow redevelopment region downstream of the reattachment (X/D = 1.73). The algebraic turbulence models predict the reattachment point better than the k-ε model. The velocity profiles predicted with these algebraic models are in fairly good agreement with the experimentally obtained profiles at these two stations. The Chow model predictions are slightly better than those of the Baldwin-Lomax model in this flow redevelopment region. The vertical (w) component of the velocity is better predicted by the k-ε model than it is by the algebraic models both in the flow recirculation and redevelopment regions. The profiles made by the algebraic models are in especially poor agreement with the experimental data for radial positions greater than half of the base radius. Figure 2c shows the turbulent shear stress profiles in the wake. The computed values obtained by both the algebraic models and the k-ε model are compared with the experimental data. In general, a small improvement can be observed in the values predicted with the k-ε model over those predicted with the algebraic models. A discrepancy exists between the experimentally obtained turbulent shear stress and the predicted shear stresses with all of the turbulence models. This is especially true near the peaks at X/D = 1.26 and 1.42. The magnitude of the peak predicted by the k-ε model is about the same as that predicted by the Baldwin-Lomax model at these two positions; however, they both underpredict the experimental peak. The Chow model underpredicts the peak even more. As for the location of the peak, the k-ε model does better than the algebraic models. As X/D is increased from 1.26 to 1.42, the location of the peak predicted by the k-ε model shifts downward and moves closer to the center line similar to that observed in the experiment. This is not seen in the predictions made by the algebraic models. The k-ε model prediction agrees better than the predictions made by the algebraic models at X/D = 1.73.

Of particular interest is the accurate prediction or determination of base pressure and, hence, base drag. Figure 3 shows the base pressure distribution (over the base). The base pressures predicted by both the algebraic models and the two-equation k-ε turbulence model are compared with the experimental data. The experimental data are shown in dark circles and the computed results are shown in lines. The base pressures predicted by both algebraic turbulence models show a big increase near the center line of symmetry. The experimental data shows almost no change (only 3%) in the base pressure distribution. The base pressures are very poorly predicted by the algebraic models, not only near the center line but also near the base corner. A much-improved base pressure distribution is predicted by the k-ε model and its agreement with the measured base pressure is quite good. As expected, the k-ε prediction shows a small increase in the base pressure near the center line; however, it is unclear why it is not observed in the data. The average base pressure computed by the k-ε model is within 5% of the experimental value whereas the algebraic models predictions differ from the experimental value by 20–25%. Detailed analysis of the near wake flowfields and the eddy viscosities computed by these models reveal significant differences in the eddy viscosity in the free mixing shear layer region ($r/R \approx 0.4$–0.6) and the reverse velocity in the near wake near the centerline. In the shear layer where the velocity gradients are large, the algebraic models predict large eddy viscosities whereas the k-ε model predicts small values. This difference in the mixing region results in small reverse velocities in the near wake with the k-ε model and large reverse velocities with the algebraic models. This in turn results in higher stagnation pressure at the base at the centerline and a large variation of base pressure over the base. With the k-ε model, small reverse velocities in the centerline near the base result in only a small increase in the pressure as the flow stagnates and subsequently to a flatter pressure variation over the base. The k-ε computations generally required 50% more computational time than the algebraic model predictions.

Conclusions

A zonal, implicit, time-marching Navier-Stokes computational technique has been used to compute the turbulent supersonic base flow over a cylindrical afterbody. Flowfield computations have been performed at M_∞ = 2.46 using two algebraic models and a two-equation k-ε turbulence model.

Comparison of both the mean and turbulence quantities have been made with the available experimental data. Both algebraic turbulence models predict the mean velocity components poorly in the recirculatory flow region in the wake. In general, the velocity components predicted by the two-equation k-ε model are in better agreement with the experimental data than those predicted by the algebraic models. Computed base pressure distributions have been compared with the measured base pressures. The base pressures predicted by the algebraic models show a much larger variation and are in worse agreement with the data. The measured base pressures show a very small change along the base and are predicted rather well with the k-ε turbulence model.

References

[1]Sahu, J., Nietubicz, C. J., and Steger, J. L., "Navier-Stokes Computations of Projectile Base Flow With and Without Base Injection," *AIAA Journal*, Vol. 23, No. 9, 1985, pp. 1348–1355.

[2]Herrin, J. L., and Dutton, J. C., "An Experimental Investigation of the Supersonic Axisymmetric Base Flow Behind a Cylindrical Afterbody," Univ. of Illinois at Urbana-Champaign, UILU 91-4004, Urbana, IL, May 1991.

[3]Baldwin, B. S., and Lomax, H., "Thin-Layer Approximation and Algebraic Model for Separated Turbulent Flows," AIAA Paper 78-257, Jan. 1978.

[4]Chow, W. L., "Improvement on Numerical Computation of the Thin-Layer Navier-Stokes Equation—With Special Emphasis on the Turbulent Base Pressure of a Projectile in Transonic Flight Condition," Univ. of Illinois at Urbana-Champaign, CR No. DAAG29-81-D-0100, Urbana, IL, Nov. 1985.

[5]Chien, K. Y., "Predictions of Channel and Boundary-Layer Flows with a Low-Reynolds-Number Turbulence Model," *AIAA Journal*, Vol. 20, No. 1, 1982, pp. 33–38.

Demonstration of an Elastically Coupled Twist Control Concept for Tilt Rotor Blade Application

R. C. Lake,* M. W. Nixon,† M. L. Wilbur,*
J. D. Singleton,* and P. H. Mirick†
NASA Langley Research Center,
Hampton, Virginia 23681

Introduction

GIVEN the complex, directional nature of composite materials, as well as the complicated structural design requirements associated with advanced tilt rotor blade designs, many problems arise in the development of extension-twist-coupled tilt rotor blades. Foremost among these is the lack of an extensive analytical/experimental database for elastically coupled structures. As such, significant amounts of basic research directed toward developing a better understanding of the fundamental problems inherent in new design concepts are required. For example, the effects of pretwist on the extension, bending, and torsional behavior of anisotropic beams with nonhomogeneous, irregular cross sections were investigated in Ref. 1. Numerical results indicated that the torsional stiffness in the one- and two-cell designs varied as a function of pretwist magnitude, decreasing for moderate levels of pretwist while increasing for high pretwist levels, when the

Presented as Paper 92-2468 at the AIAA/ASME/ASCE/AHS/ASC 33rd Structures, Structural Dynamics, and Materials Conference, Dallas, TX, April 13–15, 1992; received July 11, 1992; revision received Aug. 11, 1993; accepted for publication Oct. 26, 1993. This paper is declared a work of the U.S. Government and is not subject to copyright protection in the United States.

*Research engineer, MS 340. Member AIAA.
†Research engineer, MS 340.